Exp Fluids (2011) 50:429–441
DOI 10.1007/s00348-010-0944-7

RESEARCH ARTICLE

Thermal characteristics of the wake shear layers from a slightly heated circular cylinder

J. Mi · M. Xu · R. A. Antonia · J. J. Wang

Received: 15 February 2010 / Revised: 16 June 2010 / Accepted: 16 July 2010 / Published online: 4 August 2010

Abstract In this paper, we investigate the thermal characteristics of wake shear layers generated by a slightly heated circular cylinder. Measurements of the fluctuating temperature were made in the region $x/d = 0.6$ to $x/d = 3$ (where x is the downstream distance from the cylinder axis and d is the cylinder diameter) using a single cold-wire probe. The Reynolds number Re was varied in the range 2,600–8,600. For $Re = 5{,}500$, simultaneous measurements were made with a rake of 16 cold wires, aligned in the direction of the mean shear, at $x/d = 2$ and 3. The results indicate that the passive temperature can be an effective marker of various instabilities of the wake shear layers, including the Kelvin–Helmholtz (KH) instability. The temperature data have confirmed the approximate Re^m dependence of the KH instability frequency (f_{KH}) with different values of m over different ranges of Re, as reported previously in the literature. However, it is found that this power-law dependence is not exact, and a third-order polynomial dependence appears to fit the data well over the full range of Re. Importantly, it is found that the wake shear-layer instabilities can be grouped into three categories: (1) one with frequencies much smaller than the Bénard–Kármán-vortex shedding frequency, (2) one associated with the vortex shedding and (3) one related to the KH instability. The low-frequency shear-layer instabilities from both sides of the cylinder are in-phase, in contrast to the anti-phase high-frequency KH instabilities. Finally, the observed streamwise decrease in the mean KH frequency provides strong support for the occurrence of vortex pairing in wake shear layers from a circular cylinder, thus implying that both the wake shear layer and a mixing layer develop in similar fashion.

J. Mi (✉) · M. Xu
State Key Laboratory of Turbulence & Complex Systems and Department of Energy & Resources Engineering, College of Engineering, Peking University, 100871 Beijing, China
e-mail: jcmi@coe.pku.edu.cn

R. A. Antonia
Discipline of Mechanical Engineering, Faculty of Engineering, University of Newcastle, Newcastle, NSW 2308, Australia

J. J. Wang
Institute of Fluid Mechanics, Beijing University of Aeronautics and Astronautics, 100191 Beijing, China

1 Introduction

The wake of a circular cylinder placed normal to a uniform stream has long been the subject of extensive studies. A characteristic feature of the flow is the periodic shedding of Bénard-Kármán vortices rolled up by the separated shear layer from either side of the cylinder in the region $x/d = 2$–3. There is a significant influence of Reynolds number (Re) on the characteristics of the shear layer and the vortex formation zone. Based on the nature of the separated shear layer, Zdravkovich (1997) subdivided the wake into several flow regimes: i.e., the shear layer may be laminar, transitional or turbulent, which, in turn, influences the formation of the Bénard–Kármán vortices.

The instability of the shear layer separating from either side of a cylinder has been put in evidence in quite a number of previous studies (e.g., Bloor 1964; Gerrard 1978; Wei and Smith 1986; Kourta et al. 1987; Norberg 1987, 1998; Prasad and Williamson 1997a, b; Rajagopalan and Antonia 2005; Thompson and Hourigan 2005) and has been described in the literature under various names, e.g. the 'Bloor–Gerrard' instability, the 'secondary-vortex'

instability, the Kelvin–Helmholtz (KH) instability and the shear-layer (SL) instability. We simply label it the KH instability. Bloor (1964) first discovered that the KH instability manifested itself as high frequency bursts in hot-wire signals when the Reynolds number Re ($\equiv U_1\ d/\nu$, where U_1 is the free-stream velocity, d the cylinder diameter and ν the viscosity) exceeded 1,300 and obtained the following dependence on Re of the ratio of the KH frequency (f_{KH}) to the shedding frequency (f_V) of the Bénard–Kármán vortices

$$f_{KH}/f_V \sim Re^m, \tag{1}$$

where the exponent m is a constant. Assuming similarity between the wake shear layer and the plane mixing layer, she also found that m was approximately 0.5 when Re varied between 5,000 and 25,000. The KH instability was later observed for $Re \geq 350$ by Gerrard (1978), who also provided support for $m = 0.5$. However, Wei and Smith (1986), who determined the value of f_{KH} from hot-wire measurements and from flow visualizations, obtained significantly different values of m (0.87 and 0.773). In contrast, the hot-wire measurements and flow visualizations of Kourta et al. (1987), who used a cylinder with end plates, revealed a distribution for f_{KH}/f_V similar to that of Bloor (1964). Mihailovic and Corke (1997), using measurements in the range $Re = 3{,}500$–$5{,}300$, reported a value of $m = 0.5$. On the other hand, Prasad and Williamson (1997a) made a compilation of hot-wire data from seven shear-layer studies (including those of Bloor and Wei & Smith) and obtained, from a least-squares fit to the data, an exponent of $m = 0.67$, viz.

$$f_{KH}/f_V = 0.0235\, Re^{0.67}, \tag{2}$$

over the range $1{,}200 \leq Re \leq 100{,}000$. Their empirical analysis based on the variation of the base pressure coefficient and shear-layer momentum thickness provided plausible support for the $Re^{0.67}$ dependence. Further support for this value of m was provided by the more recent data of Brede (2004) for $5{,}000 \leq Re \leq 20{,}000$ and Rajagopalan and Antonia (2005) for $740 \leq Re \leq 14{,}800$ who considered their data together with all previously available data. Nevertheless, the latter authors indicated that, when their data are examined in isolation, two different ranges could be identified: (i) $m = 0.72$ for $Re < 5{,}000$ and (ii) $m = 0.67$ for $Re > 5{,}000$. These results are consistent with the conclusions of Norberg (1987, 1998) and Prasad and Williamson (1997b) that the wake shear flow exhibits a basic change near $Re = 5{,}000$. Such a transition could be due to the vortex shedding being less organized for $Re > 5{,}000$ than for $Re < 5{,}000$. Very interestingly as well, after re-examining the data obtained by Prasad and Williamson (1997a) and Norberg (1987), Thompson and Hourigan (2005) claimed that m is determined by the boundary-layer properties at separation, as suggested by Bloor (1964), but with a slightly higher value than 0.5 over two discrete ranges of Re. They obtained that $m \approx 0.584$ over $1{,}500 \leq Re \leq 5{,}000$ and $m \approx 0.546$ for $10{,}000 \leq Re \leq 50{,}000$. In this context, there is not yet consensus for the Re dependence of f_{KH}/f_V. The present work provides a new set of fluctuating temperature data immediately downstream of a slightly heated circular cylinder.

In the near wake immediately downstream from a cylinder, only little information is available on the KH vortex pairing which, if present, should be readily identified by the spectral peaks around $f_{KH}/2$. Hot-wire measurements at $x/d \approx 0.2$ and $y/d \approx 0.7$ by Ahmed and Wagner (2003) for $Re = 29{,}000$, 33,000 and 45,000 indeed indicated the presence of such peaks, thus suggesting the occurrence of the vortex pairing in a wake shear layer in a similar manner to a mixing layer. This was also observed by Rajagopalan and Antonia (2005) for smaller values of Re. Such observations seem consistent with the early numerical simulations of Braza et al. (1990), who used two-dimensional (2-D) large-eddy simulation (LES) for $Re = 2{,}000$–$10{,}000$ and reported discernible subharmonics of f_{KH} found in pressure–frequency spectra of the cylinder shear layer. However, the measurements of Wei and Smith (1986) and Unal and Rockwell (1988a, b), as well as the LES results of Jordan (2003), did not exhibit any subharmonics of f_{KH} at almost any (x, y) location in the very near wake. Unal and Rockwell (1984) and Chyu and Rockwell (1996a) thus eliminated the possibility of pairing in a wake shear layer. They argued that, in contrast to free jets and mixing layers, the small-scale KH vortices from a cylinder do not merge to generate larger vortices in the shear layer, because the presence of the re-circulating zone in the wake prevents KH vortex merging. In a wake, such a pairing was observed only when it was forced at f_{KH} (Chyu and Rockwell 1996b; Mihailovic and Corke 1997). On the other hand, when the formation of Bénard-Kármán vortices was suppressed by inserting a downstream splitter plate, streamwise pairing of the KH vortex structures and the associated subharmonics appeared immediately as in a free shear mixing layer (Unal and Rockwell 1984). This may imply that pairing occurs only when the shear layer is isolated. Unal and Rockwell (1984) concluded that the growth of the KH vortices is independent of large-scale Bénard–Kármán vortices and, as a result, the development of the wake shear layer differs intrinsically from that of a single, isolated shear layer where vortex merging is often observed. Hence, given the 'conflicting' observations indicated above, it is quite clear that there is some unresolved or missing mechanism(s) for the pairing of the wake KH vortices to take place.

The above-cited investigations indicated that the KH fluctuations are intermittent. Wei and Smith (1986) speculated that this intermittency is due to the transverse motion of the shear layer caused by the Bénard–Kármán vortex shedding. This, however, was ruled out later by several investigations (e.g., Cardell 1993; Prasad and Williamson 1997a). Cardell (1993) pointed out that, if it were the case, the transverse shear-layer motion would cause a stationary probe to only periodically 'feel' fluctuations from the KH instability. The measurements of Prasad and Williamson (1997a) showed that the amplitude of a transverse motion is less than 8% of the thickness of the shear layer and also that the transverse motion diminishes as one travels upstream in the shear layer. These authors concluded from a detailed analysis of their data and other previous measurements that "the observed intermittency in shear-layer fluctuations is not caused by the transverse motion of the shear layer, but is principally the result of a random streamwise motion of the transition point, which is influenced by temporal changes in near-wake three-dimensional structures." They also deduced from their own flow visualizations (their Fig. 11) that the shear-layer (or KH) instability is in-phase across the wake, a claim made by Gerrard (1978) as well. Although these authors did not make it clear, they seemed to suggest that the KH vortices on both sides of a cylinder occur simultaneously and also in-phase, because the vortices result from the high-frequency shear-layer instability that they referred to. Whether or not this is the case, however, has yet to be ascertained. This has provided a natural motivation for the present work.

The previous measurements were made using either hot-wire/LDA/PIV (velocity) or flow-visualization techniques. To the best of our knowledge, no previous study on the KH instability has been done using a passive temperature signal, especially simultaneous temperature measurements in the near wake of a slightly heated cylinder. The use of passive temperature, which acts as a marker of structures in a turbulent flow, has proved to be very effective and, in some cases, helped to emphasize particular flow features more clearly than velocity-based data. For example, the existence of large-scale temperature discontinuities in a turbulent boundary layer and other shear flows has permitted detailed studies of the properties related to the large-scale organization in these flows, e.g. Chen and Blackwelder (1978), Sreenivasan et al. (1979), Antonia et al. (1979). These spatially coherent discontinuities have been closely linked to the small-scale anisotropy of a passive scalar, e.g. Sreenivasan and Antonia (1997) and Warhaft (2000). The present overall objective is to investigate the thermal characteristics of the wake shear layer from a slightly heated, circular cylinder. Specifically, we address the following issues

(1) Can the passive scalar capture the features of the KH instability and Bénard–Kármán vortices in the near wake of a slightly heated circular cylinder effectively? And can the scalar data confirm relation (1) with possibly a more accurate value of m or at least a value of m that exhibits less scatter than in earlier studies?
(2) Is pairing of the KH vortices from a circular cylinder always possible or does it occur only under some very special conditions? There are few experimental investigations which reveal KH vortex pairing in the shear layers from a circular cylinder.
(3) Is the KH instability really well in-phase across the wake? Or is it only the low-frequency shear-layer oscillations from both sides of a cylinder that are well in phase?

The wake shear layer starts to roll up into a Bénard–Kármán vortex street within 2–3 diameters of the cylinder and the flow is subsequently dominated by the vortex street. The present study focuses on the very near wake ($x/d < 3$) before the vortex street has been completely formed.

2 Experimental details

The present temperature measurements were made in the quasi-two-dimensional turbulent wake of a circular cylinder. Experiments were carried out in an open-return low-turbulence wind tunnel with a 2,400 mm long working section (350 × 350 mm). The bottom wall was tilted to achieve a zero streamwise pressure gradient. The cylinder of diameter $d = 12.7$ mm was installed in the mid-plane and spanned the full width of the working section, 200 mm from the exit plane of the contraction. As a result, there was a blockage of about 3.6% and an aspect ratio of 27.6. The cylinder was heated electrically to a level which is sufficiently small for the temperature differential (10–20°C) above ambient to be treated as a passive scalar. Because the initial free stream was very uniform and of low turbulence, the temperature variation over the cylinder surface was small (<1°C). Measurements were made at constant free-stream velocities between $U_o = 3.1$ m/s and $U_o = 10.2$ m/s; correspondingly, the Reynolds number varied between $Re = 2{,}630$ and $Re = 8{,}600$. In the free stream, the longitudinal and lateral turbulence intensities were about 0.05 and 0.08% of U_o, respectively. In addition, under the above conditions, the momentum thickness was estimated to be about 6 mm regardless of the magnitude of Re.

The instantaneous temperature, above ambient, Θ ($= < \Theta > + \theta$, where $< \Theta >$ is the mean value and θ is the fluctuation) was measured using both a single cold-wire probe located at $x/d = 0.6$–3 and a rake of 16 cold wires

fixed at $x/d = 2$ and 3 (see Fig. 1, Table 1). The cold wires (diameter = 1.27 μm) were made of Wollaston (Pt-10%Rh) wire with etched lengths of about 1 mm. Each of these wires was operated with a circuit at low constant current (=0.1 mA). For this magnitude of the current, the sensitivity of the wires to velocity fluctuations was negligible. The cold-wire signals from the circuits were offset, amplified and then digitized using a 12-bit A/D board (analogue to digital converter) and the data were stored on a PC for further processing. Sampling frequencies of 3.2–3.5 kHz were used after low-pass filtering at 1.6–1.75 kHz for all values of *Re,* and each record had a duration of about 40–60 s.

Since the primary objective is to investigate the thermal characteristics of the separating shear layer over a range of Reynolds numbers, detailed cold-wire measurements were made only in the very near-wake region by moving the single probe along the x and y-directions ($x/d = 0.6$–3 and $y/d = -1.0$ to 1.0) and also by placing the rake of 16 cold wires at $x/d = 2$ and 3 (Table 1 shows their values of y/d) to investigate the correlation between the shear layers from both sides of the cylinder.

3 Results and discussion

3.1 Dependence of the KH instability on downstream and transverse distances

Previous work has conclusively revealed that, as *Re* increases to beyond a critical value of Re_{cr} ($\approx$350–3,000; the magnitude depending on a few parameters, see Wu et al. 1996), the thin and contorted shear layers which separate from either side of a cylinder often flap indiscriminately in the lateral (y) direction and generate a series of small-scale KH vortices. At a given Reynolds number $>Re_{cr}$, the location of the onset of instability moves arbitrarily in the streamwise direction (Prasad and Williamson 1997a). This is indeed what is

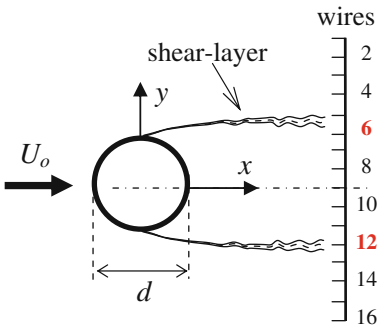

Fig. 1 Schematic arrangement of the cylinder, the coordinate system and the rake of 16 cold wires

Table 1 The y-locations of the 16 cold wires for $x/d = 2$ and 3

Wire no.	($x/d = 2$) y/d	($x/d = 3$) y/d
1	1.6	1.21
2	1.43	1.04
3	1.22	0.83
4	1.00	0.61
5	0.78	0.39
6	0.58	0.19
7	0.39	−0.004
8	0.16	−0.23
9	−0.01	−0.40
10	−0.17	−0.56
11	−0.4	−0.79
12	−0.62	(broken)
13	−0.89	−1.28
14	−1.09	−1.48
15	−1.33	−1.72
16	−1.5	−1.89

observed in the present measurements of the fluctuating temperature (θ) at $Re = 2{,}800$–$8{,}600$. Figures 2a and b illustrate the time traces of θ obtained with a single cold-wire probe for $Re = 5{,}500$ and $x/d = 0.6$–2.5 at the y-location (Y_{KH}), where the KH instability can be detected effectively, and for $Re = 3{,}200$ and $x/d = 2$ at $y/d = 0$–0.79. It is clear from Fig. 2a ($Re = 5{,}500$) that the shear layer, which is initially laminar, i.e., with no instability occurring locally (thus leading to very smooth θ signals), oscillates due to the downstream formation of the Bénard–Kármán vortices and at $x/d \approx 0.6$ starts to fluctuate intermittently at a high frequency. This results in the formation of small-scale bursting fluctuations or the wavelet patch in $\theta(t)$, corresponding to the KH instability. As x increases up to $x/d = 1.5$, the wavelet patch (indicated by arrows) becomes more pronounced and widespread. At $x/d = 2$, some of the large-scale Bénard–Kármán vortices have formed completely and travel downstream together with the small-scale KH vortices. Further downstream at $x/d \geq 3$, the Bénard–Kármán vortex street is well established, and the KH vortices are no longer evident. Figure 2a also shows unambiguously that the small-scale bursting fluctuation is superimposed on the large-scale fluctuations caused either by the shedding of Bénard–Kármán vortices or by some low-frequency shear-layer oscillation.

The y-dependence of the KH instability can be seen from the θ signals in Fig. 2b for $Re = 3{,}200$ and $x/d = 2$. Clearly, the KH instability of the separated boundary layer is observed in $\theta(t)$ measured approximately between $y/d = 0.5$ and $y/d = 0.8$. It appears that the separated boundary layer oscillates around $Y_{KH} \approx 0.65$ and the

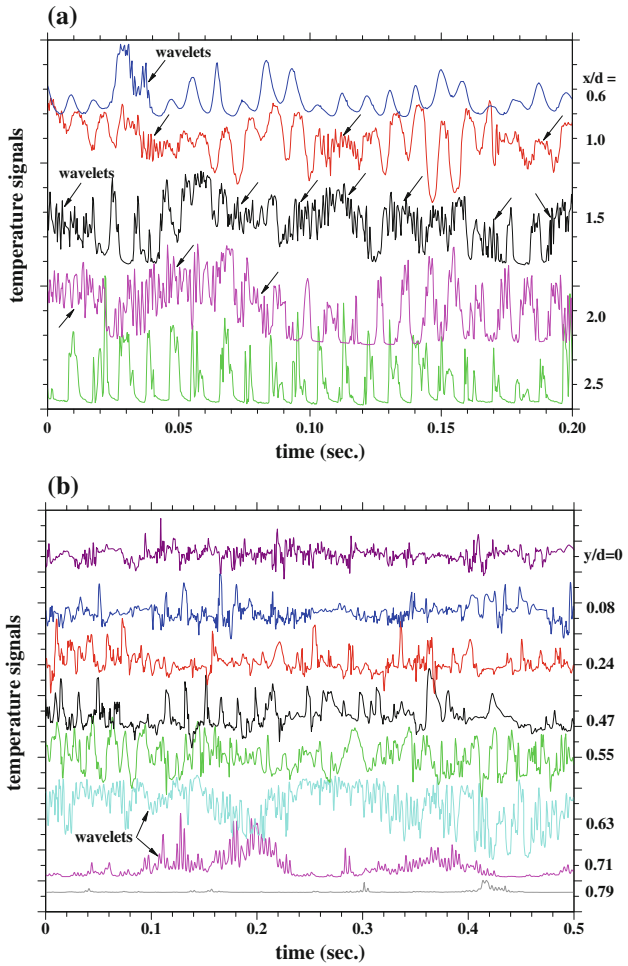

Fig. 2 Fluctuating signals of temperature (θ) obtained by a single cold wire. **a** $Re = 5{,}500$ and $x/d = 0.6$–2.5 and at a y-location where the instability can be detected effectively; **b** $Re = 3{,}200$ and $x/d = 2$ at $y/d = 0$–0.79

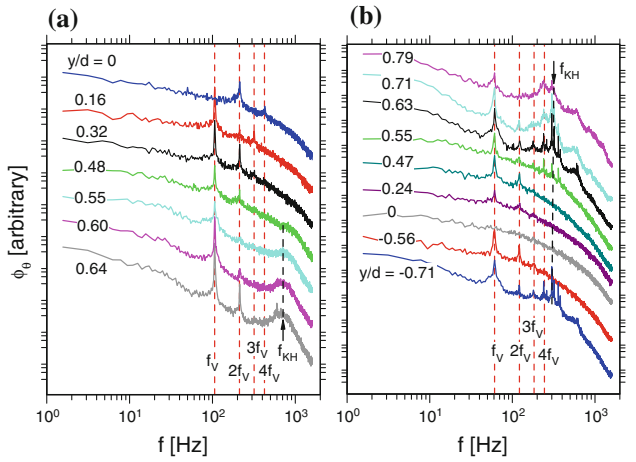

Fig. 3 Frequency spectra of the fluctuating temperature (θ) for **a** $Re = 5{,}500$ and $x/d = 1.5$ and **b** $Re = 3{,}200$ and $x/d = 2$

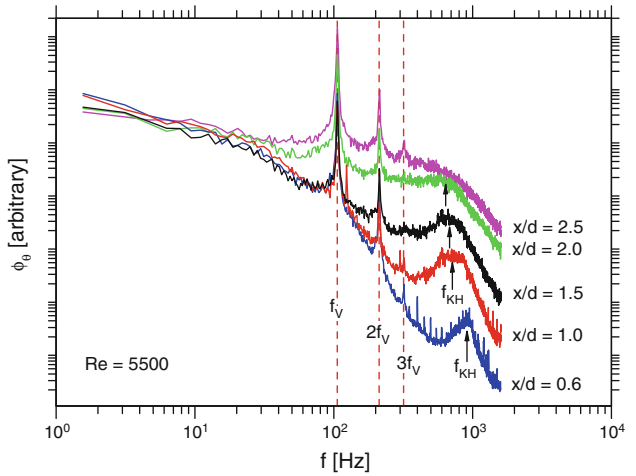

Fig. 4 Frequency spectra of the fluctuating temperature (θ) for $Re = 5{,}500$ and $x/d = 0.6$–2.5

transverse amplitude is about $\pm 0.15d$ for this case. This can be seen also from the corresponding frequency spectra of $\theta(t)$, denoted by Φ_θ (f). Figures 3a and b, respectively show Φ_θ across the wake at $x/d = 1.5$ for $Re = 5{,}500$ and that at $x/d = 2$ for $Re = 3{,}200$. There are distinct peaks in Φ_θ that are unmistakably associated with the shedding of Bénard–Kármán vortices at f_V and its harmonics, and also with the KH instability at f_{KH}. It is evident that the measured mean value of f_{KH} virtually does not vary with the y-location where the cold-wire probe could sense the wake shear layers.

To examine the streamwise evolution of the KH instability frequency, Fig. 4 displays Φ_θ corresponding to $\theta(t)$ presented in Fig. 2a. There are distinct peaks due to the shedding of the large-scale vortices at $f_V \approx 102$ Hz and its harmonics and also to the small-scale KH vortices travelling with the frequency f_{KH}. Evidently, as the shear layers proceed downstream, f_{KH} decreases from 930 Hz at $x/d = 0.6$ to 640 Hz at $x/d = 2$. This decrease is associated with KH vortex merging (and will be discussed further in Sect. 3.3). Note also that the KH instability occurs occasionally or intermittently at $x/d = 2.5$ and thus a distinct-related peak cannot be discerned in Φ_θ.

3.2 Effect of the Reynolds number Re

As Re increases, the Bénard–Kármán vortices are formed at a higher rate (f_V) and simultaneously the KH instability occurs more rapidly (f_{KH}). These can be demonstrated by comparing the θ spectra for $Re = 3{,}200$ (Fig. 3b), where $f_V \approx 60$ Hz and $f_{KH} \approx 304$ Hz, with those for $Re = 5{,}500$ (Fig. 3a), where $f_V \approx 102$ Hz and $f_{KH} \approx 750$ Hz. Previous investigations, using either hot wire, LDA, PIV (velocity) or flow-visualization techniques, generally support relation (1), i.e., $f_{KH}/f_V \sim Re^m$, but m varies between 0.5 and 0.87.

To check this using the temperature measurements, Figs. 5 and 6 show, respectively the spectra Φ_θ against f/f_V for $Re = 2{,}800$–$8{,}500$ and the ratio f_{KH}/f_V versus Re. The present data of f_{KH}/f_V are plotted, over a wider range of Re, together with those from Bloor (1964), Gerrard (1978), Wei and Smith (1986), Kourta et al. (1987), Prasad and Williamson (1997a), Norberg (1987) and Rajagopalan and Antonia (2005), in Fig. 6a and with three selected data sets from Prasad and Williamson, Norberg, and Rajagopalan and Antonia in Fig. 6b. Apparently, the present result agrees well with Eq. (2) obtained by Prasad and Williamson, i.e., $f_{KH}/f_V = 0.023Re^{0.67}$. Like most of the previous data, the present data do not support $m = 0.5$ proposed by Bloor (1964). The reason for this is explored below.

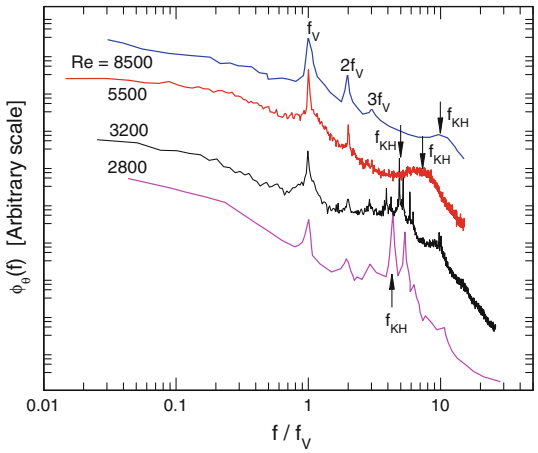

Fig. 5 Frequency spectra (Φ_θ) of the fluctuating temperature (θ) for different Reynolds numbers varying between $Re = 2{,}800$ and 8,500

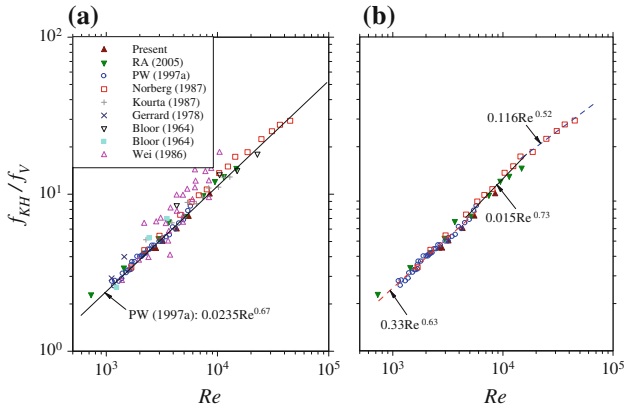

Fig. 6 Variation of f_{KH}/f_V with the Reynolds number. **a** Ten sets of previous data shown together with $f_{KH}/f_V = 0.023Re^{0.67}$, as obtained by Prasad and Williamson (1997a); **b** four sets of recent data and three power-law fits of $f_{KH}/f_V \sim Re^m$ for $Re \leq 5{,}000$, $Re = 5{,}000$–$10{,}000$, and $Re = 10{,}000$–$50{,}000$. Note that RA and PW on part (**a**) stand for Rajagopalan & Antonia and Prasad & Williamson, respectively

It has been an open question for several decades whether the origin and development of mixing layers and wake shear layers are similar. In a mixing layer, stability analysis (Michalke 1965) and measurements have shown that f_{KH} scales on the initial boundary-layer thickness δ, which yields $f_{KH} \propto Re^{1.5}$ since $\delta \propto Re^{0.5}$. In a wake, both f_{KH} and f_V are strongly dependent on Re and the mixing layer type analysis of Bloor (1964) resulted in a $Re^{0.5}$ dependence for f_{KH}/f_V. However, most of the available data have yielded a value of m greater than 0.5. For instance, Wei and Smith (1986) argued that it is the shear-layer momentum thickness in the linear growth zone which should be the appropriate length scale rather than the thickness of the boundary layer at separation, which may explain their large value (0.87) of m. The analysis of Prasad and Williamson (1997a), based on the shear-layer thickness and some physical arguments, yielded

$$f_{KH}/f_V \sim \left[\frac{(1 - C_{Pb})^{1/2}}{S(\beta\, Re^{-1/2} + 1)^{1/2}}\right] Re^{0.5} \sim Re^{0.69} \tag{3}$$

where C_{Pb} is the base pressure coefficient dependent on Re, S ($\equiv f_V d/U_\infty$) is the Strouhal number associated with the Bénard–Kármán vortex shedding and β is an experimental constant (≈ 100). Obviously, Eq. (3) is consistent with $m = 0.67$ obtained by best fitting of all the then available data in the literature, including their own.

More recently, Rajagopalan and Antonia (2005) observed that there are two different regimes: (i) an $Re^{0.72}$ dependence for $Re < 5{,}000$ and (ii) an $Re^{0.67}$ dependence for $Re > 5{,}000$. This suggests that a transition may occur near $Re = 5{,}000$ and thus reinforces the conclusions of Norberg (1987, 1998) and Prasad and Williamson (1997b) that the wake shear flow exhibits a basic change near $Re = 5{,}000$. Norberg (1998) and Rajagopalan and Antonia (2005) believed that such a change is associated with the less organized vortex shedding at $Re > 5000$, compared to the case for $Re < 5000$, which will be discussed later.

Almost at the same time, Thompson and Hourigan (2005), after re-examining the data of Prasad and Williamson (1997a) and Norberg (1987), observed that the exponent m is only slightly greater than 0.5 over two separate ranges of Re. These authors, using the boundary-layer properties at separation, obtained the following relationship:

$$f_{KH}/f_V \sim \left[\frac{(1 - C_{Pb})^{1/2}}{Sf(\theta_o)}\right] Re^{0.5} \tag{4}$$

where $f(\theta_o)$ accounts for the variation due to the movement of the separation angle of the shear layer, θ_o, with Reynolds number. Analysing the Re dependence of the parameters in the square brackets, they obtained $m \approx 0.584$ over $1{,}500 \leq Re \leq 5{,}000$ and $m \approx 0.546$ for $10{,}000 \leq Re \leq 50{,}000$.

These values agree well with their best-fit values (0.57 ± 0.04 and 0.52 ± 0.06) for the two ranges from the data of Prasad and Williamson (1997a) and Norberg (1987). Based on the data of Norberg (1987, 1994) for S, C_{Pb} and their numerical simulation for $f(\theta_o)$ at 90°, they argued that a single value of m cannot apply over the entire range of Re.

To check the above suggestions of Rajagopalan and Antonia (2005) and Thompson and Hourigan (2005), Fig. 6b presents our data together with those of Prasad and Williamson (1997a), Norberg (1987) and Rajagopalan and Antonia (2005). Note that these three data sets are selected here because we believe that the corresponding experiments were undertaken with great care, producing consistent data with very little scatter and also in good agreement in the regions of overlap. The result of Fig. 6b appears to provide support for Thompson and Hourigan (2005) if we apply power-law fits to the data over the ranges identified by these authors. Seemingly, the relation $f_{KH}/f_V \sim Re^m$ works well over the three ranges: (i) $m = 0.63$ for $Re \leq 5{,}000$; (ii) $m = 0.73$ for $5{,}000 \leq Re \leq 10{,}000$; and (iii) $m = 0.52$ for $10{,}000 \leq Re \leq 50{,}000$. Range (i) is the same as Thompson and Hourigan and Rajagopalan and Antonia for $Re < 5{,}000$ and range (iii) is similar to range 2 of Thompson and Hourigan, while range (ii) is the transition range of Thompson and Hourigan. The exponent (0.63) obtained presently for the range (i) is slightly higher than that of Thompson and Hourigan (0.57) but smaller than that of Rajagopalan and Antonia (0.72), perhaps, due to more data involved for the best fitting. Note that the present work identifies range (ii) where $f_{KH}/f_V \sim Re^{0.73}$ is approximately valid over the range $Re = 5{,}000$–$10{,}000$.

However, a very careful inspection finds that all the data in Fig. 6b do not strictly obey the relationship $f_{KH}/f_V \sim Re^m$ over any range of Re. That is, the above division of the three regimes for Re^m, that of the two regimes by Thompson and Hourigan (2005) or Rajagopalan and Antonia (2005), or that for the entire range (i.e., $f_{KH}/f_V = 0.023Re^{0.67}$) of Prasad and Williamson (1997a) should be considered only as being three approximate options. Figure 7a shows that, using a third polynomial, all the four data sets can be very well fitted together over the entire measured range ($Re = 740$–$50{,}000$). This best-fit curve, viz.

$$f_{KH}/f_V = 1.38 \times 10^{-13} Re^3 - 2.1 \times 10^{-8} Re^2 + 1.29 \times 10^{-3} Re + 1.36 \quad (5)$$

looks quite similar (see Fig. 7b) to the Re dependences of

$$S^{-1}(1 - C_{Pb})^{1/2}(\beta Re^{-1/2} + 1)^{-1/2}$$

and $(1 - C_{Pb})^{1/2}/[Sf(\theta_o)]$.

The latter quantities (Eqs. (3) and (4), respectively) are estimated from the measured C_{Pb} and S of Norberg (1987, 1994) and the data of β and $f(\theta_o)$ of Prasad and Williamson (1997a) and Thompson and Hourigan (2005), respectively. This similarity may be regarded as evidence for the validity of (5), but not $f_{KH}/f_V \sim Re^m$, for the entire range of Re. Figure 7b evidently demonstrates that the Re dependence of the combined factors square bracketed in Eq. (3) or (4) is not in a power-law form. Hence, should Eqs. (3)–(4) and the data of Norberg (1987, 1994) all be correct, the relation $f_{KH}/f_V \sim Re^m$ will not strictly hold over any range of Re.

3.3 KH vortex pairing in the shear layer

Vortex pairing is often deduced from flow visualizations and by the presence of a subharmonic peak in spectra of hot-wire signals at f_{KH}. Vortex pairing in a mixing layer is well known and can be significantly enhanced by exciting the flow at suitable frequencies (Husain et al. 1988). Despite the similarity between the mixing layer and near-wake shear-layer development, there is very little information on the possibility of vortex pairing in the wake. Norberg (1987) observed spectral amplitudes near the subharmonic component of f_{KH} to be only slightly larger (Fig. 7 of his report). Unal and Rockwell (1988a) suggested that the absolute instability dominates the near wake and injects a significant amount of turbulent energy at the vortex shedding frequency. Their spectra did not exhibit subharmonics of f_{KH}, which is in contrast to what is observed in a mixing layer. However, when the large-scale Karman-vortex formation is suppressed by inserting a splitter plate, vortex pairing and subharmonic components were observed (Unal and Rockwell 1988b). As the splitter plate was separated sufficiently from the cylinder, vortex pairing was no longer observed. Unal and Rockwell thus concluded that the large amplitude fluctuations induced by

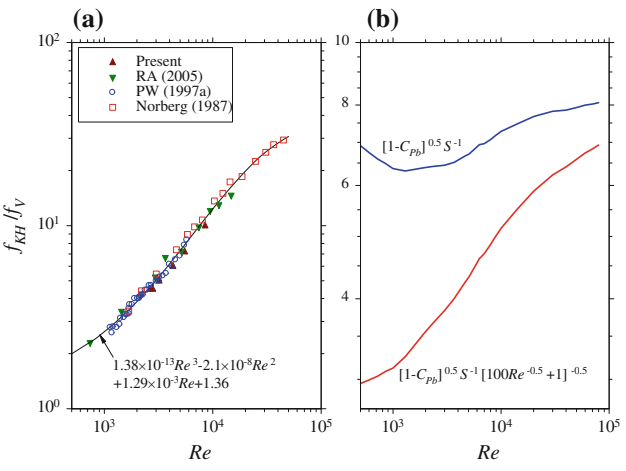

Fig. 7 The Reynolds number dependences of (**a**) f_{KH}/f_V and (**b**) combined factors within square-brackets in Eq. (3) or (4). Note that RA and PW on part (**a**) stand for Rajagopalan & Antonia and Prasad & Williamson, respectively

the formation of Karman vortices preclude the pairing of KH vortices and that the growth of these vortices is independent of the Karman vortices and, as a result, the development of the wake shear layer differs intrinsically from that of a single, isolated shear layer where vortex merging is observed.

The pairing of KH vortices in a wake has been observed when suitable excitation is applied to the wake. Chyu and Rockwell (1996b) observed a collective coalescence, like a mixing layer, when the flow was excited at subharmonic components of f_{KH}. In a forced wake, Mihailovic and Corke (1997) observed peaks in the spectra at $f_{KH}/2$. Excitation had very little influence on the shedding frequency f_V. Without excitation, Ahmed and Wagner (2003) appear to have observed spectral peaks at f_{KH} and $f_{KH}/2$. In their work, a single hot wire was placed quite close to the cylinder surface at $x/d = 0.2$ and $y/d = 0.1$. At $Re = 29{,}000$, 33,000 and 45,000, they observed two peaks, whereas at $Re = 97{,}000$, only a single peak at f_{KH} was observed. Moreover, Rajagopalan and Antonia (2005) showed through the u spectra that the presence of spectral peaks at $f_{KH}/2$ at various Reynolds numbers for $Re = 3{,}700$–$14{,}800$, in addition to peaks at f_V and $2f_V$. In some cases, they also observed a peak at $2f_{KH}$. These authors noticed that, at low Reynolds numbers, the subharmonic component could not always be identified unambiguously in the spectra. In this case, before a full development of the shear layer, Karman vortices are formed, which tend to inhibit the vortex pairing. At very high Reynolds numbers, an early break-down to turbulence occurs and, hence, vortex pairing can hardly be discerned. Nevertheless, Rajagopalan and Antonia (2005) concluded that, without external excitation, vortex pairing and breakdown can be identified in a wake shear layer as for a mixing layer from spectral peaks at $f_{KH}/2$ and $2f_{KH}$ and also that the near-wake zone develops via a convective instability mechanism before strong Karman vortices dominate the flow.

The present temperature spectra Φ_θ plotted in Figs. 3, 4, 5 show no subharmonic peaks near $f_{KH}/2$. However, this does not exclude the possibility of the KH vortex pairing or merging because there is no need for each set of adjacent vortices to merge thus producing subharmonic peaks in Φ_θ at $f_{KH}/2$. In the context of establishing whether vortex pairing exists, it may be more appropriate to examine the streamwise variation of f_{KH}. If pairing does occur (not necessarily for all the KH vortices), then the number of KH vortices will reduce and thus f_{KH} will decrease as x increases. Figure 7 clearly demonstrates that, as the downstream distance increases from $x/d = 0.6$ to $x/d = 2$, the spectrum Φ_θ varies significantly. In particular, the broad peak (centred approximately at $f_{KH} = 930$ Hz at $x/d = 0.6$) associated with the KH vortices shifts to the left; correspondingly, the peak centres at $f_{KH} \approx 720$, 680 and 640 Hz for $x/d = 1.0$, 1.5 and 2.0, respectively. This shift is not due to a variation in the **transverse** location of the probe, as indicated by Figs. 3a and b for $Re = 5{,}500$ and $x/d = 1.5$ and $Re = 3{,}200$ and $x/d = 2$. Note also that, while f_{KH} decreases significantly from $x/d = 0.6$ to $x/d = 1.0$, its further decrease at larger x/d is quite small. The decrease in f_{KH} is obviously caused by vortex pairing, which nevertheless occurs mainly at $x/d < 1$, i.e., quite close to the cylinder. Accordingly, taken together with the results of Rajagopalan and Antonia (2005) and Ahmed and Wagner (2003), we understand that the pairing of the KH vortices in the shear layer of a circular cylinder is always possible without external excitation.

3.4 Correlations of the shear-layer oscillations from both sides of a cylinder

Prasad and Williamson (1997a) made a note from their flow visualizations (their Fig. 11) that "the shear-layer instability appears to be in-phase across the wake". However, these authors did not clarify whether "the shear-layer instability" is a high-frequency (small-scale) or low-frequency (large-scale) instability or both. Our interpretation of their results is that the KH vortices on both sides of a cylinder occur simultaneously and in phase. Prasad and Williamson noted that "although such in-phase behaviour was observed in the majority of our photographs, other configurations did manifest themselves." One may therefore ask whether or not the KH vortices on both sides of a cylinder occur concurrently if the intermittent shear-layer instability is "in-phase across the wake". Another question that arises is whether the in-phase instabilities on both sides of a cylinder can drive the entire near wake to oscillate in phase.

To address the questions raised above, we used a rake of 16 cold wires aligned in the y-direction at $x/d = 2$, shown early in Fig. 1. Figure 8 displays 0.26-second time traces of the fluctuating temperature (θ) obtained simultaneously at nine y-locations between $y/d \approx -0.9$ and 0.8, from wire 5 to 13. Wires 5 and 13 were located almost completely in the free stream, while during most of the record duration, wires 6 and 12 were apparently located inside the shear layers from the top and bottom sides of the horizontal cylinder, respectively. The signals $\theta_6(t)$–$\theta_{12}(t)$, from wires 6 to 12, except $\theta_9(t)$ ($y \approx 0$), all clearly show oscillations due to the shedding of Bénard–Kármán vortices. Inspection of these signals leads to the following observations:

- The largest-scale shear-layer (SL) oscillations, as exhibited in $\theta_6(t)$ and $\theta_{12}(t)$, respectively, appear to be in phase. To demonstrate this better, we plotted in

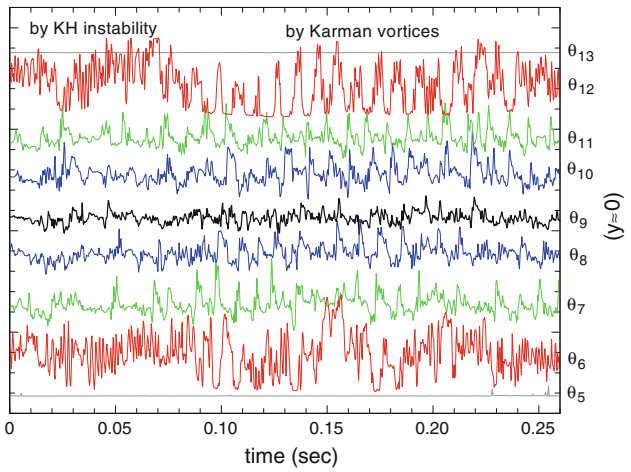

Fig. 8 Signals of the fluctuating temperature (θ) obtained simultaneously at $-0.9 < y/d < 0.6$ ($Re = 5{,}500$ and $x/d = 2$)

Fig. 9 the two signals over a longer duration (1.2 s). Indeed the in-phase behaviour of the low-frequency SL oscillation is more evident in Fig. 8. This result, to our understanding, coincides with the point made by PW and Gerrard (1978) that the SL instability is "in-phase across the wake". However, this SL oscillation is not their high-frequency SL or KH instability that may generate the small-scale vortices at the frequency of f_{KH}.

- The fluctuations of $\theta_6(t)$ and $\theta_{12}(t)$ due to the Bénard–Kármán vortex shedding are, as expected, nearly in anti-phase, i.e., with a phase difference of $\Psi = 180°$ (π radians). This is because the shedding alternates on either side of the cylinder.
- The fluctuations of $\theta_{11}(t)$ and $\theta_{12}(t)$ due to the Bénard–Kármán vortex shedding appear to be just about in anti-phase ($\Psi \approx 180°$) as are those of $\theta_6(t)$ and $\theta_7(t)$. This is a little surprising because each pair of signals came from adjacent cold wires on the same side with a separation of $\sim 0.2d$ in the y-direction.

To quantify these observations more generally, we calculated the overall and three band-pass (f_1–f_2) time-delay (τ) correlation coefficients, $\rho_{i-j}(\tau)[f_1 : f_2]$, between $\theta_{12}(t)$, as a reference, and other $\theta(t)$ signals, viz.

$$\rho_{i-j}(\tau)[f_1 : f_2] = \frac{<\theta_i(t)[f_1 : f_2]\theta_j(t+\tau)[f_1 : f_2]>}{<\theta_i^2>^{1/2}<\theta_j^2>^{1/2}}$$

where $i = 12$ (reference) and $j = 6$–11 represent the wire numbers, and f_1 and f_2 are the lower and upper frequency band limits, respectively. Note that the original θ signals were obtained at the cut-off frequency of 1,750 Hz. Here, the present pass-band and stop-band edge frequencies (in Hz) are selected to be $(f_1, f_2) = (0, 20)$, (20, 220) and (500, 800), with a view to quantifying the cross-correlations between θ_{12} and other signals resulting, respectively from the low-frequency global SL oscillation, the Bénard–Kármán vortex shedding and the KH instability.

Figures 10, 11, 12, 13 show, respectively, the corresponding results of $\rho_{i-j}(\tau)[f_1 : f_2]$ over the three band-pass regions and those for the entire band (0, 1,750). Overall, the cross-correlation results support the above observations (1)–(5) made from instantaneous signals. A more specific analysis follows. Fig. 10 shows the time-delay (τ) correlation coefficients of the low-frequency (0–20 Hz) temperature fluctuations from wire 12 and those from the other wires, denoted by $\rho_{12-j}(\tau)[0 : 20]$. The coefficient $\rho_{12-6}(\tau)[0 : 20]$ exhibits a maximum value (≈ 0.75), while $\rho_{12-j}(\tau)[0 : 20]$ shows a minimum ($\approx -0.15 \sim -0.45$), approximately at $\tau = 0$. This suggests that the largest-scale fluctuations of θ_{12} and θ_6, or low-frequency oscillations of the two shear layers, which are not likely to be caused by the Bénard–Kármán vortex shedding, are strongly (phase) correlated. By comparison, the correlations between the

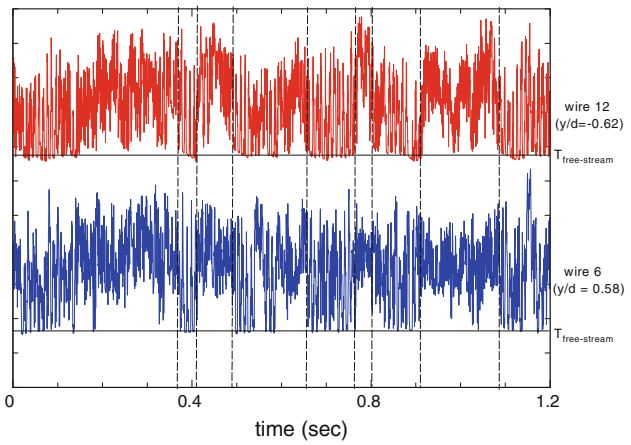

Fig. 9 Signals of the fluctuating temperature (θ) obtained simultaneously at $y/d \approx \pm 0.6$ ($Re = 5{,}500$ and $x/d = 2$)

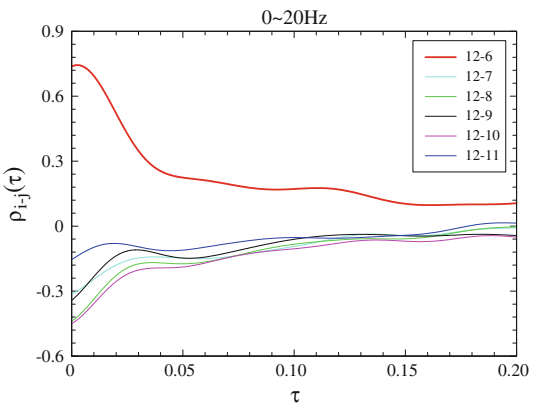

Fig. 10 The time-delay correlation coefficients of the low-frequency (0–20 Hz) temperature fluctuations from wire 12 and those from the other wires ($Re = 5{,}500$ and $x/d = 2$)

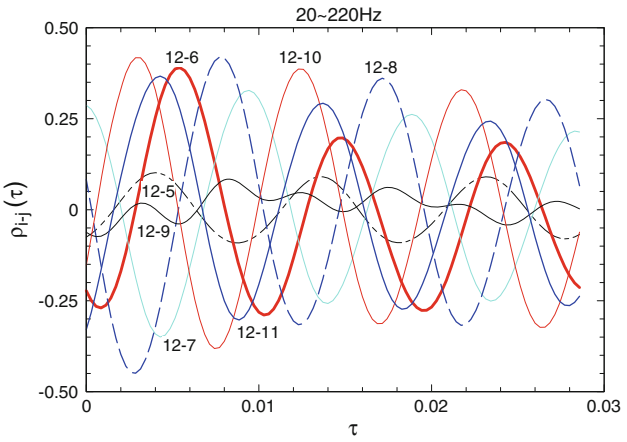

Fig. 11 The time-delay correlation coefficients of the medium-frequency (20–220 Hz) temperature fluctuations from wire 12 and those from the other wires ($Re = 5{,}500$ and $x/d = 2$)

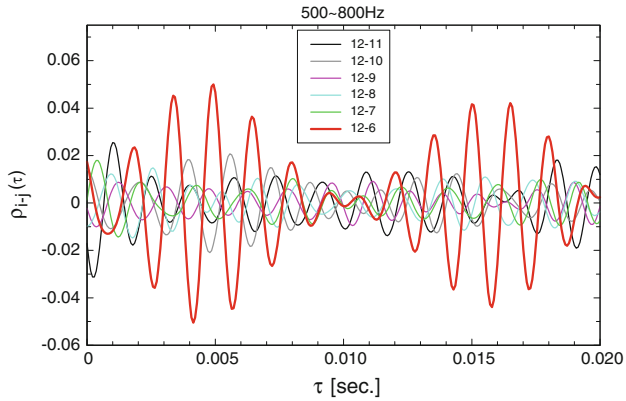

Fig. 12 The time-delay correlation coefficients of the high-frequency (500–800 Hz) temperature fluctuations from wire 12 and those from the other wires ($Re = 5{,}500$ and $x/d = 2$)

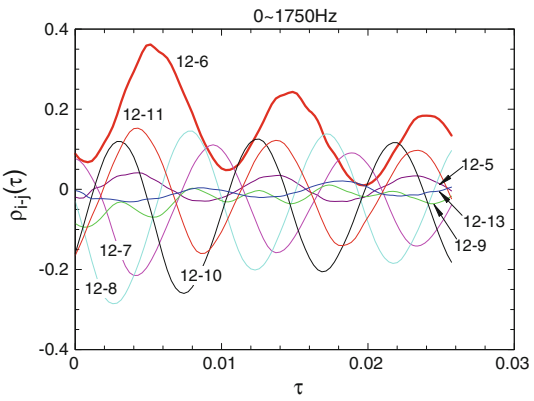

Fig. 13 Overall time-delay correlation coefficients between the temperature fluctuations from wire 12 and those from the other wires ($Re = 5{,}500$ and $x/d = 2$)

lowest-frequency fluctuation of θ_{12} and those from the other wires are significantly weaker while the slowest fluctuations of signals θ_7–θ_{11} occur roughly in anti-phase with those of θ_6 and θ_{12}. This is indeed the case, as demonstrated in Fig. 14 by the phase difference $\Psi_{12\text{–}j}[f_1 : f_2]$ between θ_{12} and θ_6–θ_{11} over the band-pass region [0:20 Hz]. Hence, it is deduced that the lowest-frequency instabilities of the two shear layers are indeed in-phase with each other, but in anti-phase with those from the region between the shear layers (see Figs. 10, 14). In contrast, the fluctuations associated with the vortex shedding ($f_V \approx 102$ Hz) contribute differently to the overall correlation between θ_{12} and θ_j, as reflected in $\rho_{12-j}(\tau)[20 : 220]$ and $\Psi_{12\text{–}j}[20 : 220]$. Fig. 11 shows the variation of $\rho_{12-j}(\tau)[20 : 220]$ with τ. Consistently with $f_V \approx 102$ Hz, just over 3 complete fluctuations occur in $\rho_{12-j}(\tau)[20 : 220]$ over $\tau = 0.03$ s, reflecting the same number ($\approx$2.9) of shedding cycles. As expected, the alternate shedding of Bénard–Kármán vortices causes the fluctuations of the two shear layers to be nearly in anti-phase and thus the phase difference is nearly equal to π (Fig. 14). Interestingly, however, the phase differences between θ_{12} and either θ_{11} or θ_7 are approximately 0.9π and 2.0π, respectively. This is likely the result of the flapping motion of the thin shear layers caused by the vortex shedding. As illustrated schematically in Fig. 14, the two 'hot' shear layers strongly flap in phase and sweep over wires 6 and 11 or wires 12 and 7, nearly simultaneously. When the thin 'hot' shear layer passes over wire 12(6), wire 11(7) is exposed to a relatively cooler air stream induced by the shedding, and vice versa. As a result, $\rho_{12-11}(\tau)[20 : 220]$ takes a minimum at $\tau = 0$, which is $\rho_{12-11}(0)[20 : 220] = -0.33$, see Fig. 10. Moreover, Fig. 12 shows the high-frequency fluctuation of

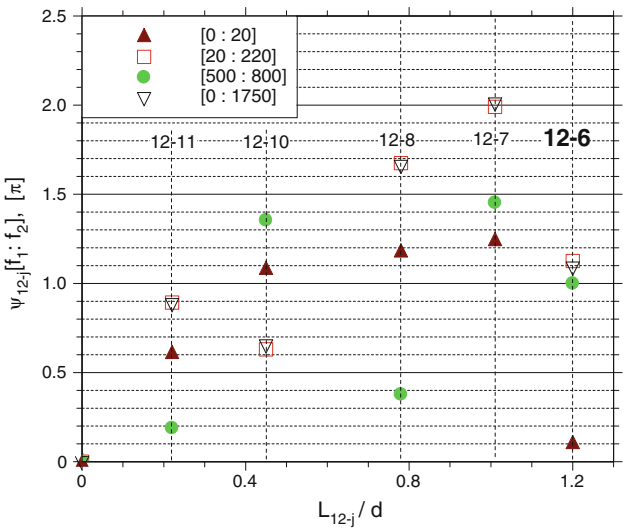

Fig. 14 Phase differences between θ_{12} and θ_6–θ_{11} for different frequency band-pass regions at $Re = 5{,}500$ and $x/d = 2$

$\rho_{12-j}(\tau)[500:800]$. As expected, generally, θ_{12} has very weak correlations (−0.02 to 0.02) with all other signals except θ_6 in terms of their high-frequency fluctuations. The slightly stronger fluctuation of $\rho_{12-6}(\tau)[500:800]$ is due to the KH instability of the two shear layers. The fact that $\rho_{12-6}(\tau)[500:800]$ takes a local maximum approximately at $\tau = 0$ might suggest that the KH instabilities from the two shear layers sometimes occur roughly concurrently or temporally locally in phase, which is evident also in Fig. 8. However, the very low value of $\rho_{12-6}(0)[500:800] \approx 0.018$ should exclude the possibility that the KH instability is globally in-phase across the wake; indeed, $\Psi_{12-6}[500:800] \approx \pi$ which means that the signals θ_6 and θ_{12} at frequencies of 500–800 Hz are globally in anti-phase. This is obviously at variance with the conjecture of Prasad and Williamson (1997a) that the high-frequency KH instability is "in-phase across the wake". A close inspection of their Fig. 11 suggests that their selected KH vortices occurring at some instant in time from both cylinder sides appear to be only very roughly in phase. This is similar to what we found by inspecting the simultaneous signals θ_6 and θ_{12}: high-frequency fine-scale bursting fluctuations are often discerned in θ_6 and θ_{12} almost simultaneously (see Fig. 8), but they are not exactly in phase, so that the phase difference $\Psi_{12-6}[500:800] \approx \pi$ and the zero-time-delay cross-correlation coefficient $\rho_{12-6}(0)[500:800] \approx 0.017$ is very small.

Based on the above results of Figs. 8, 9, 10, 11, 12, 13, 14, the shear-layer oscillations or instabilities can be placed into three groupings: i.e., (1) those with frequencies much lower than f_V ($\approx$102 Hz for the present case of $Re = 5{,}500$), denoted by the "slow SL" oscillation; (2) those due to the Bénard-Kármán-vortex shedding typically at f_V; and (3) those due to the Kelvin–Helmholtz (KH) instability with a mean frequency equal to f_{KH} and significantly greater than f_V. These are characterized in Figs. 15, 16 by the correlation coefficients between θ_{12} and θ_6 over the different frequency bands indicated above. Obviously, the overall coefficient $\rho_{12-6}(\tau)[0:1570]$ is controlled by the Bénard–Kármán vortex shedding (also see Fig. 13). It also seems obvious that the occurrence of the KH instability is somehow associated with the Bénard–Kármán vortex shedding, although this issue is beyond the scope of the present study.

As the flow proceeds further downstream from $x/d = 2$, the Bénard–Kármán vortices begin to alternate on either side of the cylinder and, concurrently, the shear layers vanish. Subsequently, these coherent structures travel downstream in the anti-symmetric mode, commonly denoted as the 'Bénard–Kármán vortex street'. At $x/d = 3$, the street largely dominates the flow and the vortices generated from one side make deep excursions into the other side, so that the mean flow in the central region

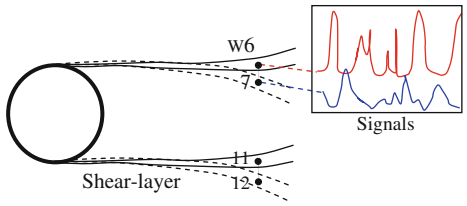

Fig. 15 Schematic of the shear-layer flapping, due to the Karman-vortex shedding at f_V, as reflected in the θ signals from wire pairs 6–7 and 11–12 placed at $x/d = 2$

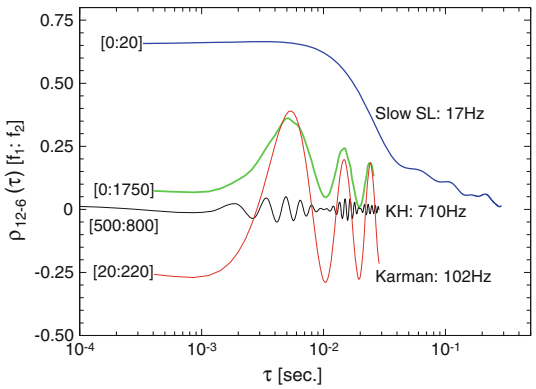

Fig. 16 The time-delay correlation coefficients between temperature fluctuations from wires 12 and 6 over different frequency bands (indicated on plot)

behaves in a coherent manner. As a result, the cross-correlation $\rho_L(\tau = 0)$ between the fluctuating temperatures from two symmetric locations with respect to the centreline remains positive even when the separation distance L exceeds d, as shown in Fig. 17. By comparison, the flow upstream of $x/d = 2$ is more complicated due to the interactions between the shear layers, reverse flow motions, and the Bénard–Kármán vortex shedding. Since the alternating shedding controls the very near wake, the negative value of $\rho_L(\tau = 0)$ is obtained for $L < d$ (see Fig. 17). The positive correlation of $\rho_L(\tau = 0) \approx 0.1$ for $L = 1.2d$ is due to the low-frequency in-phase oscillations of the two shear layers.

4 Conclusions

To our knowledge, this is the first investigation into the behaviour of the thermal wake shear layers generated by a slightly heated circular cylinder. Cold wires were used to measure the fluctuating temperature, treated here as a passive scalar, from the very near wake at $x/d \leq 3$ for Reynolds numbers in the range 2,600 to 8,600. In particular, for $Re = 5{,}500$, simultaneous measurements across the wake were made with a rake of 16 cold wires, aligned in the direction of the mean shear, at $x/d = 2$ and 3.

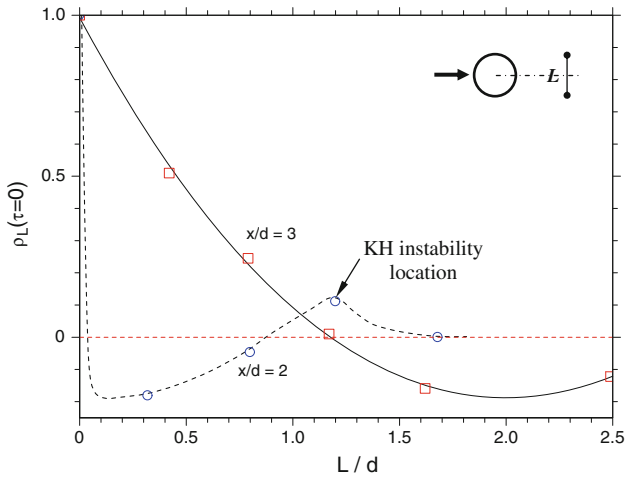

Fig. 17 The correlation coefficients of the temperature fluctuations obtained from two locations, separated by L, approximately symmetrical about the centreline

Use of a passive scalar has proved to be quite effective in marking various instabilities of the wake shear layers, including the Kelvin–Helmholtz (KH) instability. We have observed the intermittency in the shear-layer fluctuations, as found previously by, for example, Norberg (1987) and Cardell (1993). The present measurements have also confirmed that the relationships $f_{KH}/f_V \propto Re^{0.67}$, proposed by Prasad and Williamson (1997a), as well as $f_{KH}/f_V \propto Re^{0.57}$ for $Re = 1{,}500$–$5{,}000$ and $f_{KH}/f_V \propto Re^{0.52}$ for $Re = 10{,}000$–$50{,}000$, suggested by Thompson and Hourigan (2005), are only good approximations. Strictly, however, the function $f_{KH}/f_V = f\,(Re)$ is unlikely to have a piecewise power-law form, due to the complexity of the wake shear layer. It is suggested that the f_{KH}/f_V data over the range $500 \leq Re \leq 50{,}000$ are well represented by the third-order polynomial: $f_{KH}/f_V = 1.38 \times 10^{-13}Re^3 - 2.1 \times 10^{-8}Re^2 + 1.29 \times 10^{-3}Re + 1.36$.

Intermittent vortex pairing or merging in a wake shear layer seems to occur in a similar manner to that in a mixing layer. This has been confirmed by a streamwise decrease in the KH instability frequency. Since pairing does not have to occur between each pair of adjacent KH vortices, subharmonic peaks in temperature spectra need not exist. This confirmation strengthens the argument of Rajagopalan and Antonia (2005) that the near-wake flow develops via a convective instability mechanism rather than an absolute instability mechanism.

In-phase low-frequency shear-layer oscillations from both sides of the cylinder are observed instead of the in-phase KH instabilities mentioned by Prasad and Williamson (1997a). Three types of wake shear-layer instabilities have been identified: (1) one with frequencies much smaller than the Karman-vortex shedding frequency, (2) one associated with the vortex shedding and (3) one related to the KH instability.

Acknowledgments The first author gratefully acknowledges the support for this study by the 973-project scheme (Grand No. 2007CB714601) from the Ministry of Science & Technology of China and also by Nature Science Foundation of China (Grant No. 10772006). RAA acknowledges the support of the Australian Research Council. All the authors would like to thank the referees who provided insightful comments and criticisms to an earlier version of this paper.

References

Ahmed NA, Wagner DJ (2003) Vortex shedding and transition frequencies associated with flow around circular cylinder. AIAA Jl 41(3):542–544

Antonia RA, Chambers AJ, Friehe CA, Van Atta CW (1979) Temperature ramps in the atmospheric surface layer. J Atmos Sci 36:99–108

Bloor MS (1964) The transition to turbulence in the wake of a circular cylinder. J Fluid Mech 19:290–304

Braza M, Chassaing P, Minh HH (1990) Prediction of large-scale transition features in the wake of a circular cylinder. Phys Fluids A 2:1461–1470

Brede M (2004) Measurement of turbulence production in the cylinder separated shear layer using event triggered laser-Doppler anemometry. Exp Fluids 36:860–866

Cardell GS (1993) Flow past a circular cylinder with a permeable wake splitter plate. PhD thesis, Graduate Aeronautical Laboratory, California Institute of Technology

Chen C-HP, Blackwelder RF (1978) Large-scale motion in a turbulent boundary layer: a study using temperature contamination. J Fluid Mech 89:1–31

Chyu C, Rockwell D (1996a) Evolution patterns of streamwise vorticity in the turbulent near wake of a circular cylinder. J Fluid Mech 320:117–137

Chyu C, Rockwell D (1996b) Near wake structure of an oscillating cylinder: effect of controlled shear layer vortices. J Fluid Mech 322:21–49

Gerrard JH (1978) The wakes of cylindrical bluff bodies at low Reynolds number. Proc Roy Soc A 288:351–382

Husain H, Bridges JE, Hussain F (1988) Turbulence management in free shear flows by control of coherent structures. In: Hirata M, Kasagi N (eds) Transport phenomena in turbulent flows. Hemisphere, Washington, DC, pp 111–130

Jordan SA (2003) Resolving turbulent wakes. ASME J Fluids Eng 125:823–834

Kourta A, Boisson H, Chassing P, Ha Minh H (1987) Non-linear interactions and the transition to turbulence in the wake of a circular cylinder. J Fluid Mech 181:141–161

Michalke A (1965) On spatially growing disturbances in an inviscid shear layer. J Fluid Mech 23:521–544

Mihailovic J, Corke TC (1997) Three-dimensional instability of the shear layer over a circular cylinder. Phys Fluids 9(11):3250–3257

Norberg C (1987) Effects of Reynolds number and a low intensity freestream turbulence on the flow around a circular cylinder. Publication no. 87/2, Chalmers University of Technology, Sweden

Norberg C (1994) An experimental investigation of the flow around a circular cylinder: influence of aspect ratio. J Fluid Mech 258:287–316

Norberg C (1998) LDV measurements in the near wake of a circular cylinder. In: Bearman PW, Williamson CHK (eds) Proceedings

of the ASME conference on advances in the understanding of bluff body wakes and vortex induced vibration, Washington, DC
Prasad A, Williamson CHK (1997a) The instability of a shear layer separating from a bluff body. J Fluid Mech 333:375–402
Prasad A, Williamson CHK (1997b) Three-dimensional effects in turbulent bluff body wakes. J Fluid Mech 343:235–265
Prasad A, Williamson CHK (1997c) Three-dimensional effects in turbulent bluff body wakes. Exp Therm Fluid Sci 14:9–16
Rajagopalan S, Antonia RA (2005) Flow around a circular cylinder-structure of the near wake shear layer. Exp Fluids 38:393–402
Sreenivasan KR, Antonia RA (1997) The phenomenology of small-scale turbulence. Ann Rev Fluid Mech 29:435–472
Sreenivasan KR, Antonia RA, Britz D (1979) Local isotropy and large scale structures in a heated turbulent jet. J Fluid Mech 94:745–775
Thompson M, Hourigan K (2005) The shear-layer instability of a circular cylinder wake. Phys Fluids 17(11):021702
Unal MF, Rockwell D (1984) The role of shear layer stability in vortex shedding from cylinders. Phys Fluids 27(11):2598–2599
Unal MF, Rockwell D (1988a) On the vortex formation from a cylinder. Part 1. The initial instability. J Fluid Mech 190:491–512
Unal MF, Rockwell D (1988b) On the vortex formation from a cylinder. Part 2. Control by splitter plate interference. J Fluid Mech 190:513–529
Warhaft Z (2000) Passive scalars in turbulent flows. Ann Rev Fluid Mech 32:203–240
Wei T, Smith CR (1986) Secondary vortices in the wake of circular cylinders. J Fluid Mech 169:513–533
Wu J, Sheridan J, Hourigan K, Soria J (1996) Shear layer vortices and longitudinal vortices in the near wake of a circular cylinder. Exp Therm Fluid Sci 12(2):169–174
Zdravkovich M (1997) Flow around circular cylinders, vol 1. Oxford University Press, Oxford